Relationship between Multidetector CT Imaging of the Vestibular Aqueduct and Inner Ear Pathologies

VINCENZO MAIOLO[1], GABRIELLA SAVASTIO[1], GIOVANNI CARLO MODUGNO[2], LIBERO BAROZZI[1]

[1] Radiology Department, S.Orsola-Malpighi University Hospital; Bologna, Italy
[2] ENT Department, S.Orsola-Malpighi University Hospital; Bologna, Italy

Key words: vestibular aqueduct, temporal bone, multidetector computed tomography, bony labyrinth, cochleovestibular diseases

SUMMARY – *This study investigated the relationships between morphological changes in the vestibular aqueduct (VA) in different inner ear pathologies.*
Eighty-eight patients (34 males and 54 females, ranging from seven to 88 years of age; average age 49.2 years) with cochleovestibular disorders underwent temporal bone CT (with a 64-channel helical CT system according to temporal bone protocol parameters; 0.6 mm slice thickness, 0.6 mm collimation, bone reconstruction algorithm).
All patients with cochleovestibular disorders who underwent temporal bone CT had been previously divided into six different suspected clinical classes: A) suspected pathology of the third window; B) suspected retrocochlear hearing loss; C) defined Ménière's disease; D) labyrinth lithiasis; E) recurrent vertigo. On CT images we analyzed the length, width and morphology of the VA, contact between the VA and the jugular bulb (JB), the thickness of the osseous capsule covering the semicircular canals, the pneumatization rate of the temporal bone and the diameter of the internal auditory canal. At the end of the diagnostic work-up all patients were grouped into six pathological classes, represented as follow: 1) benign paroxysmal positional vertigo (BPPV), 2) recurrent vertigo (RV), 3) enlarged vestibular aqueduct syndrome (EVAS), 4) sudden or progressive unilateral sensorineural hearing loss (SNHL), 5) superior semicircular canal dehiscence syndrome (SSCD), 6) recurrent vestibulocochlear symptoms in Ménière's disease.
We evaluated 176 temporal bones in 88 patients. The VA was clearly visualized in 166/176 temporal bones; in ten ears the VA was not visualized. In 14 ears (11 patients, in three of whom bilaterally) we found an enlarged VA while in 31 ears the VA was significantly narrower. In 16 ears a dehiscence of the JB with the vestibular or cochlear aqueduct was noted. In all six patients with suspected EVAS we found a AV wider than 1.5 mm on CT scans; moreover CT identified four patients with large VA and ill-defined clinical symptoms. Most patients with BPPV (11 patients, Class 1) we did not find any VA abnormalities on CT scans, confirming the clinical diagnosis in ten patients; in the remaining patients we found an enlarged VA, not clinically suspected. In the RV class (eight patients, Class 2) we found three patients with negative CT scans, two patients with narrow aqueduct and subsequently reclassified as Ménière's disease patients, and three patients with ectasic JB dehiscence with the VA. In patients suffering from SNHL we found no statistically significant correlation with the morphological abnormalities. The clinical suspicion of SSCD was confirmed by CT in 11/13 patients (84.6 %); in addition another seven patients showed a thinning or dehiscence of the superior semicircular canals as the prevailing alteration on CT scans, and were reclassified in this group. Ménière's disease symptoms were correlated with a VA alteration in more than half of the cases; the most striking finding in this class was that the VA was significantly narrower (21 patients).
Our study demonstrates that alterations of the VA morphology are not only related to EVAS but are also found in other inner ear pathologies such as Ménière's disease. Furthermore, MDCT may confirm the presence of correlations between the morphology of inner ear structures such as VA, semicircular canals or JB dehiscence, and alterations of vestibulocochlear function.

Introduction

Multi-detector computed tomography (MDCT) of the temporal bone has completely revolutionized the imaging of this complex region [1]. The progress achieved by the introduction of isotropic voxels with submillimetric slice thickness allowed the limitations related to partial volume artifacts and highly increased the spatial resolution to be overcome. Ongoing advances in multidetector technology improved the diagnostic accuracy in the evaluation of the temporal bone, especially in the analysis of submillimetric inner ear structures. The anatomic detail obtained through MDCT is considered more defined even than anatomical specimens, whereas dehydration effects of the tissue during fixation leads to up to 10% shrinkage of the specimen [1].

Thanks to these advantages, MDCT has permitted the recognition and characterization of inner ear anomalies not previously identified [2], resulting in an optimal technique for the investigation of middle and inner ear pathologies and evaluation of anatomical variations in preoperative assessment [3]. Many diseases, such as malformations of the cochlea, otosclerosis or ossification of the cochlea, can be diagnosed unequivocally [4,5].

MDCT also ensures an accurate analysis of the bony labyrinth, with particular regard to VA. The vestibular aqueduct (VA) is a bony canal located within the petrous portion of the temporal bone which extends behind the labyrinth, from the medial wall of the vestibule until the posterior surface of the petrous bone. It is divided in two segments: the proximal or isthmic segment and the distal segment; its morphology may be compared to an inverted "J" [6]. The VA contains the VA vein and the endolymphatic duct that posteriorly continues into the blind-ended endolymphatic sac, which is located partly in the petrous bone and partly covered by the dura mater layers [7-9]. The endolymphatic duct and sac are the non-sensory components of the membranous labyrinth, containing endolymph and connecting inside and outside the otic capsule by a narrow passage inside the VA [10].

VA enlargement is a sentinel sign for an underlying malformation of the endolymphatic duct and sac and the accuracy of this evaluation plays an important role since an aqueduct midpoint width (AMW) greater than 1.50 mm is considered to be pathognomonic for a pathological dilatation of the VA [3,11]. Narrower and shorter VA [1,12] and smaller external aperture of the VA [13] have been statistically correlated with Ménière's disease, although the overlap between normal and pathological patterns is still too wide to enable an appropriate clinical application. In up to 75% of patients, cross-sectional imaging studies may render a "normal" appearance of the labyrinth [14] and the only suspicion of alteration may be the lack of symmetry respect to the controlateral structures.

The present study aimed to analyze the relationships between anatomical conformation of the VA in different groups of cochleovestibular disorders.

Materials and Methods

Patients

We retrospectively evaluated MDCT images of the temporal bone performed during the period January 2009 to December 2011 on 88 patients with inner ear symptoms and signs diagnostic or strongly suspicious for one of the following diseases:

A) Suspected pathology of the third window: enlarged vestibular aqueduct syndrome (EVAS) or otic capsule dehiscence such as superior semicircular canal dehiscence syndrome (SCDD) or other semicirular canals dehiscence; 20 patients;

B) Suspected retrococlear hearing loss: sudden or progressive unilateral sensorineural hearing loss (SNHL); 28 patients;

C) Defined Ménière's disease according to the Committee on Hearing and Equilibrium guidelines [15]; 21 patients;

D) Labyrinth lithiasis; 11 patients;

E) Recurrent vertigo (RV), defined as an episode of RV not attributable to the other four classes, with an eventually suspected central type disease such as hemicranic vertigo [16]; eight patients.

All patients were clinically investigated with full otologic examinations in the ENT Department of our hospital: cochlear function was assessed by complete standard audiological tests (vocal and tonal audiometry to assess the type and the degree of hearing loss), tympanometry and study of stapedial reflex to exclude a middle ear pathology. Vestibular function was studied by clinical evaluation (bedside examination to search for spontaneous, positional nystagmus; the manoeuvre to identify labyrinth lithiasis; the presence of head shaking nystagmus to disclose a functional vestibular asymmetry) and vestibular tests (standardized

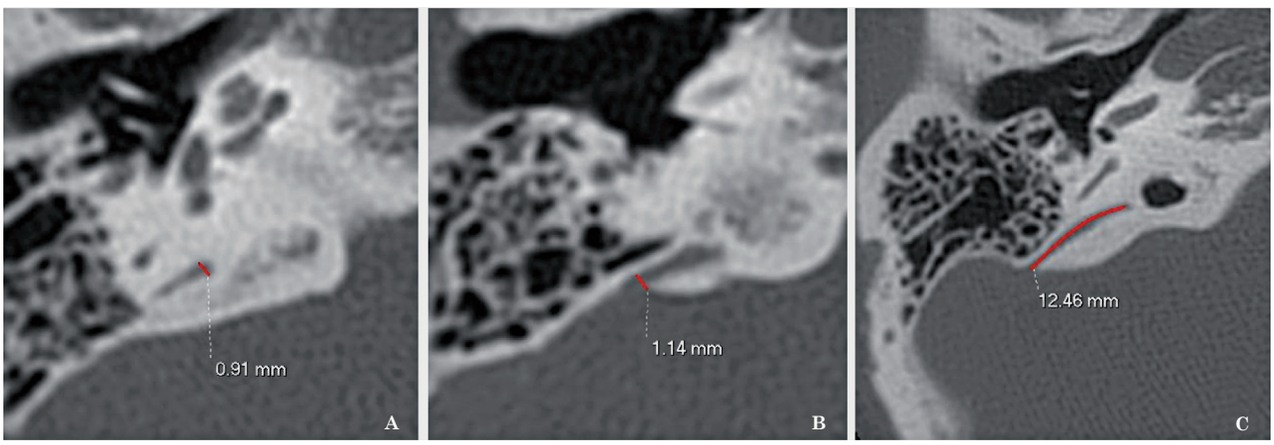

Figure 1 Axial orbitomeatal CT images with measurements of the vestibular aqueduct: A) VA width measured at the midpoint between the external aperture and common crus; B) external aperture width; C) VA length.

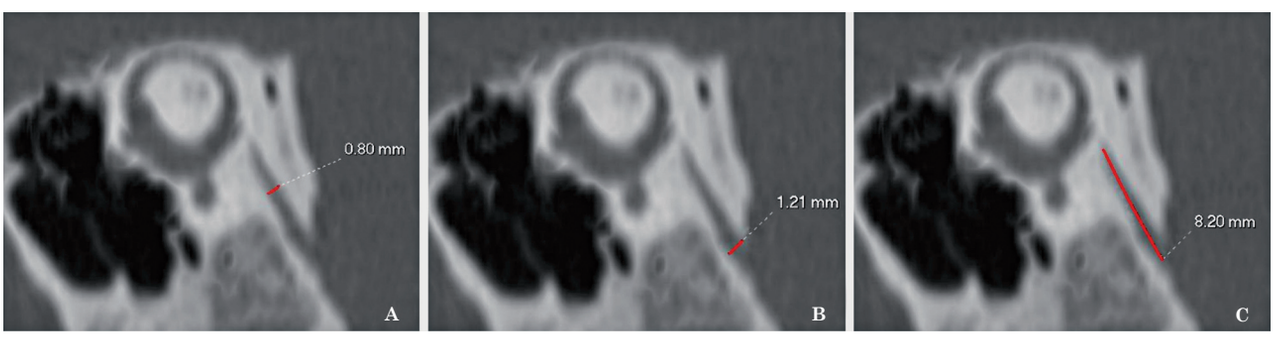

Figure 2 MPR CT images reformatted on Pöschl's plane with measurements of the vestibular aqueduct. A) VA width measured at the midpoint between external aperture and common crus; B) external aperture width; C) VA length.

bithermal caloric test to search for a deficit of the canal vestibular-oculomotor reflex) and cervical vestibular evoked potentials (C-Vemps) to study the vestibulocollic reflex and functionality of the saccule.

Patients belonging to classes B, C and E were also investigated to exclude an expansive pathology of the VIII cranial nerve or intralabyrinthine lesions, degenerative disease of the central nervous system or vascular disease responsible for clinical presentation. At the end of the diagnostic work-up all patients were grouped into six pathological classes as follows:

1) Benign paroxysmal positional vertigo (BPPV), ten patients;

2) Recurrent vertigo (RV), six patients;

3) Enlarged vestibular aqueduct syndrome (EVAS), 11 patients;

4) Sudden or progressive unilateral sensorineural hearing loss (SNHL), 18 patients;

5) Superior semicircular canal dehiscence syndrome (SSCD), 18 patients;

6) Ménière's disease, 25 patients.

Radiologic protocol - CT scanning

MDCT scans were performed with a 64-channel helical CT system (Lightspeed VCT LS Advantage 64 slices, General Electric Medical System) according to temporal bone protocol parameters: 120 kV, 225 mA, 0.5 pitch, one second rotation time, 0.6 mm slice thickness, 0.6 mm collimation, 512×512 matrix size, FOV of 16 cm, bone reconstruction algorithm. At this collimation we obtained an isotropic voxel measuring 0.6 mm on each side. In pediatric patients we reduced the radiation dose by using 120 mA for safety reasons.

The images were acquired parallel to the orbitomeatal axial plane and reconstructed in the coronal plane.

In every ear Min-IP reconstructions of the posterior and superior semicircular canals were also performed.

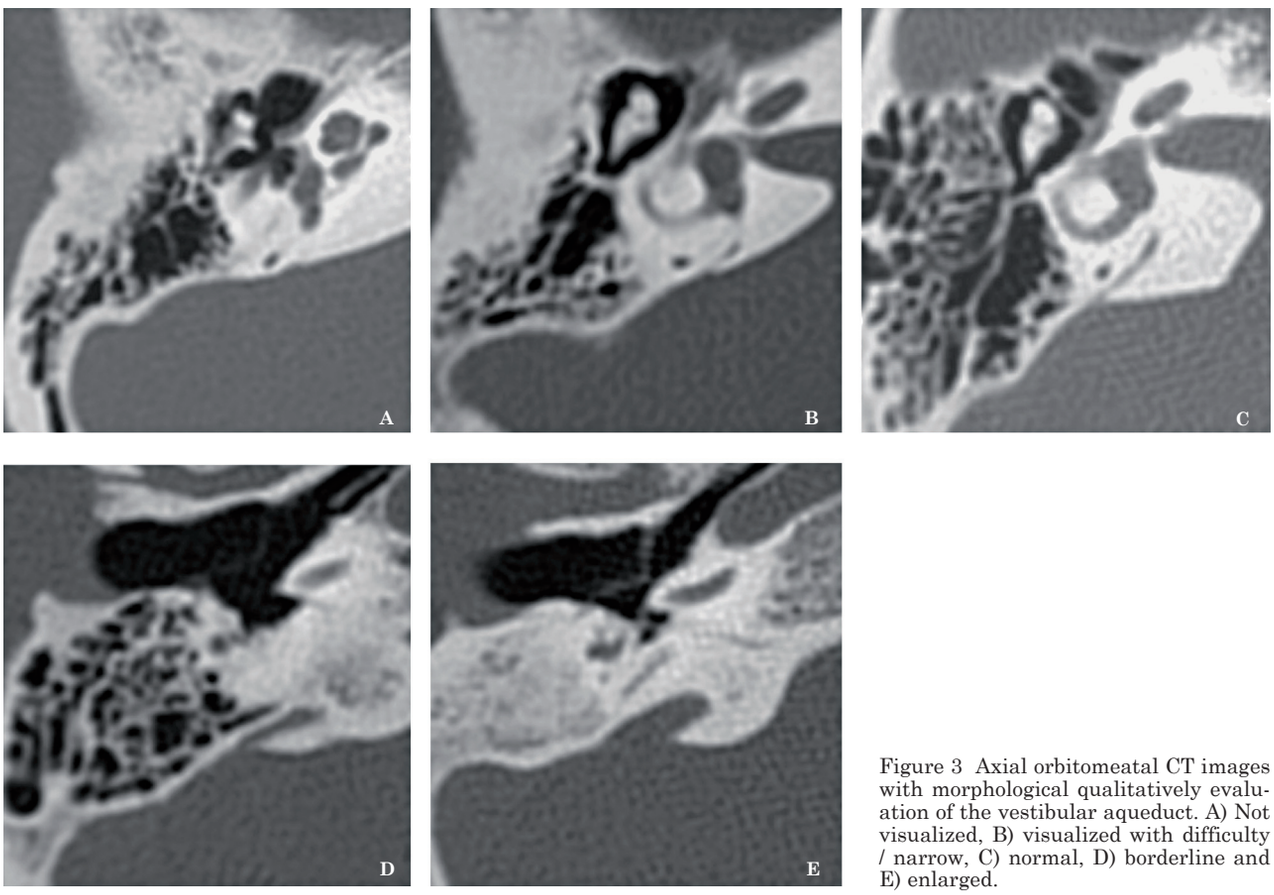

Figure 3 Axial orbitomeatal CT images with morphological qualitatively evaluation of the vestibular aqueduct. A) Not visualized, B) visualized with difficulty / narrow, C) normal, D) borderline and E) enlarged.

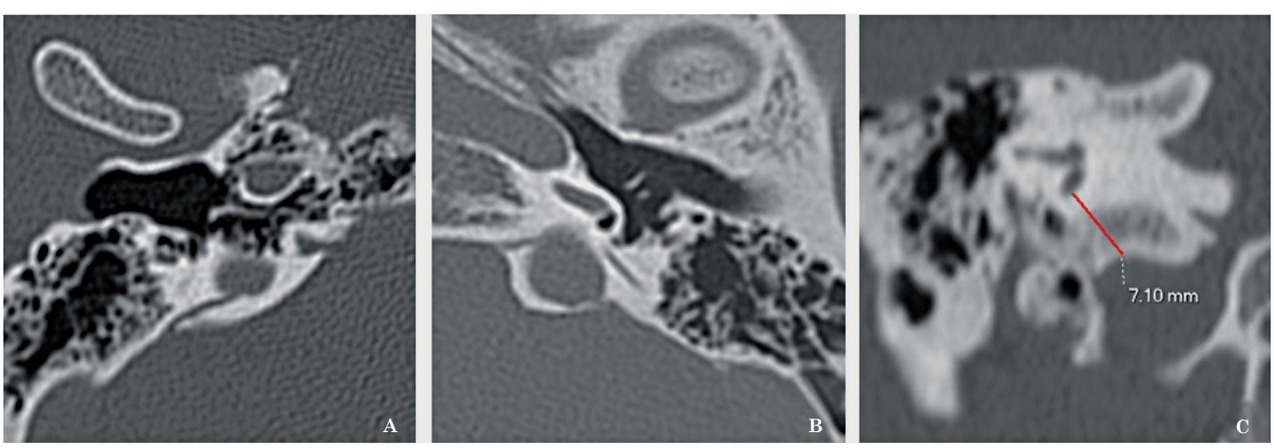

Figure 4 Axial and coronal CT images. A) Dehiscence of the jugular bulb with the vestibular aqueduct. B) 45-year-old female with recurrent dizziness not responding to drug therapy. CT images show enlarged JB dehiscent with both cochlear and vestibular aqueducts. C) Distance between jugular bulb and posterior semicircular canal bony wall.

Imaging evaluation and analyses

All images were displayed with a standardized window/level setting of 4000/300 HU using a DICOM workstation viewer. Measurements were obtained using electronic calipers and recorded in one-tenth of a millimeter units. All measurements and morphological evaluations were performed by two radiologists: one expert and one at normal level and

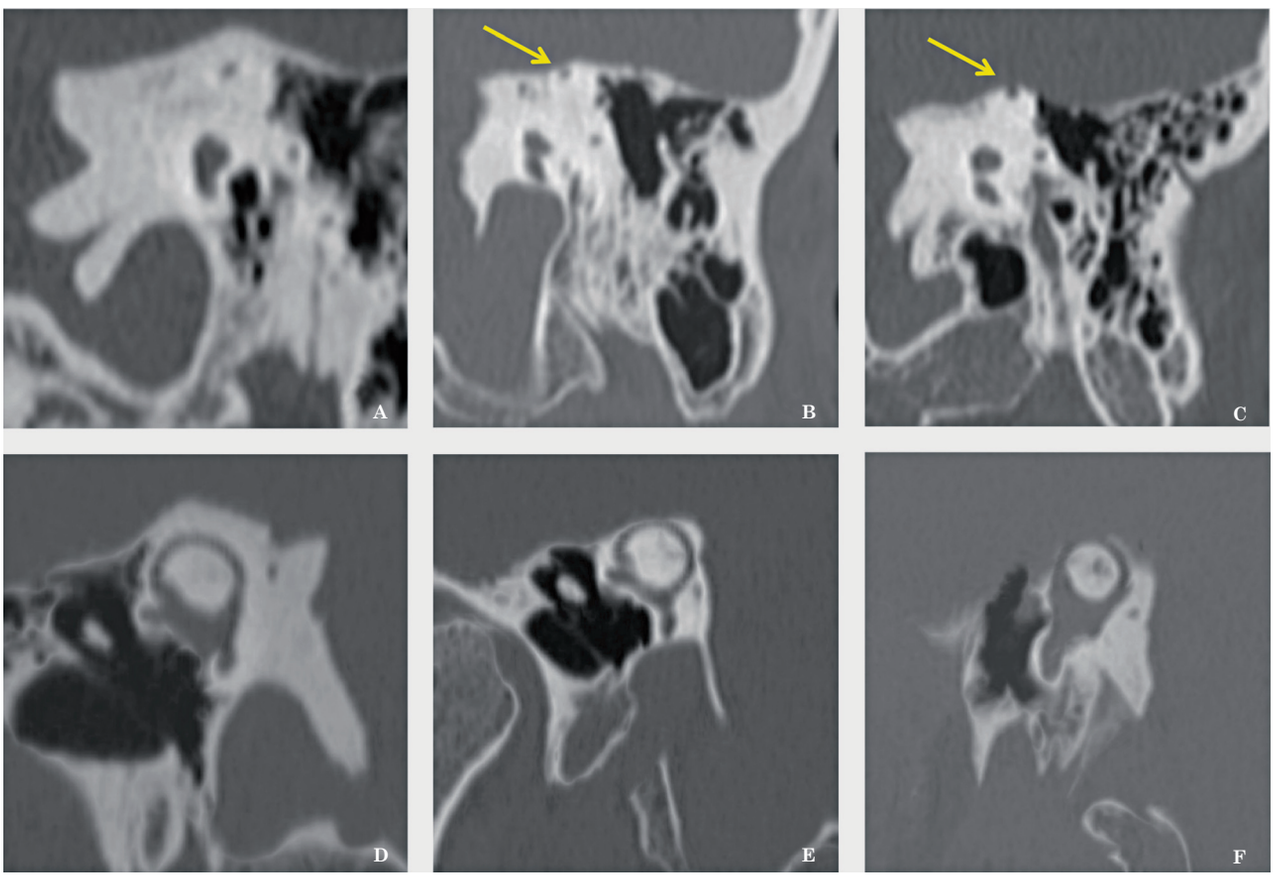

Figure 5 Coronal CT images and min-IP images reconstructed on semicircular canals with thickness evaluation. A, B) Normal condition. C, D) Thinning (arrow in C) of the osseous capsule covering the superior semicircular canal. E, F) Dehiscence (arrow in E) of the osseous capsule covering the superior semicircular canal.

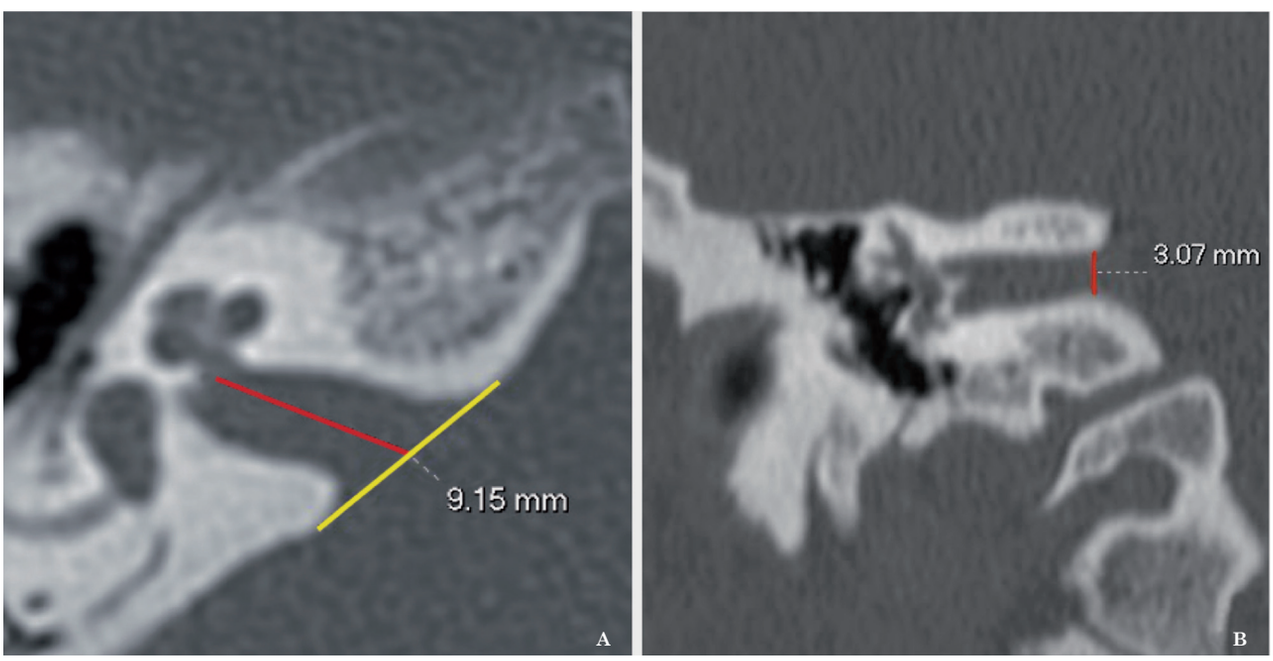

Figure 6 Axial and coronal CT images: length of the internal auditory canal (A) and diameter of the internal acoustic meatus (B).

they both agreed on the interpretation. All structures were measured independently on each side unaware of the clinical data. In all patients VA analysis was obtained by recording three measurements: VA length, VA midpoint width between the external aperture and the common crus, and VA width at the external aperture. The three values were measured both in the axial images oriented on the orbito-meatal plane and in the MPR reformatted images on the Pöschl's plane, considered to be the ideal plane to display the entire course vestibular aqueduct [17-19].

To realize reproducible measurements, all structures were analyzed in a standardized way, according to the following criteria:
– All measurements were performed excluding the bone wall;
– When it was impossible to display the VA course on a single axial image simultaneously, the midpoint between the external aperture and the common crus was visually approximated;
– VA length was measured from the vestibule to to its external opening;
– For external aperture measurement we recorded the largest width identified along an axis perpendicular to the main posterior portion of the VA.

According to the diagnostic criteria reported by Valvassori and Clemis [11], the vestibular aqueduct was considered pathologic when its diameter was 1.5 mm or greater at the midpoint, or the external aperture width was greater than 2.0 mm. We also classified the VA with a qualitative grading system according to its visibility as follows: grade 0 not visualized, grade 1 visualized with difficulty / narrow, grade 2 normal, grade 3 borderline and grade 4 enlarged.

The morphology of the external aperture was described as filiform, tubular and funnel-shaped. The pneumatization pattern of the temporal bone was classified into five types, from I to V, according to an increasing degree of pneumatization.

The relationship between VA and the jugular bulb (JB) was investigated establishing three conditions: normal JB, enlarged/ectasic JB and dehiscence of the JB with the cochlear aqueduct (CA) or VA. Additionally, the distance between the JB and the posterior semicircular canal bony wall was measured on the coronal plane.

The thickness of the osseous capsule covering the semicircular canals was analyzed, distinguishing conditions of normal thickness, thinning and dehiscence.

The internal auditory canals were explored considering the symmetry compared to the controlateral side, the length measured on the axial plane and the diameter of the internal acoustic meatus on the coronal plane.

Lastly, any malformations of the carotids or vestibulocochlear structures were excluded.

Statistical analyses

Statistical analysis was conducted in an explorative manner, based on a correlation study between two or more variables through the application of $\chi 2$ test, considering a value of $p < 0.05$ as statistically significant, and with Pearson's correlation coefficient (Pcc).

Results

VA data

We evaluated 176 temporal bones in 88 patients, divided into 34 males and 54 females (average age 49.2 years, ranging from seven to 88 years of age). The VA was clearly visualized in 166/176 temporal bones; in ten ears (5.7%; three patients bilaterally) the VA was not visualized either in the axial plane or in Pöschl's plane projection and was recorded as zero.

We established that the measurements performed on the axial projections were significantly comparable with those obtained from the Pöschl's projections ($p<0.01$ for the external aperture and $p<0.001$ for the midportion), even if the Pöschl reformats allow higher degrees of VA visualization compared with the axial scans.

VA width, VA length and external aperture width values are summarized in Table 1. No statistical relationship was noted between VA measurements and age or gender of the subjects. The external aperture widths and midpoint widths were significantly correlated to each other ($p<0.0001$). The morphological distribution of the VA was symmetric between the right and left sides ($p<0.0001$). All morphological results are summarized in Tables 2 and 3. In 14 temporal bones (7.9 %, four patients bilaterally) the VA, measured at its midpoint, was found dimensionally enlarged (>1.5 mm). The comparison of VA width and morphological evaluation showed a statistical correlation (Pcc = 0.61, $p<0.0001$) both for midpoint and external aperture measurements. There was

Table 1 Vestibular aqueduct measurements (mm)

Right Side	*Mean ± SD*	*Minimum Value (*)*	*Maximum Value*	*Median Value*
Width at the midpoint	0.876 ± 0.545	0.4	3.5	0.8
Width at the external aperture	1,218 ± 0.962	0.4	6.1	1.0
Length	5.395 ± 2.743	1.5	14.4	5.3
Left Side	*Mean ± SD*	*Minimum Value (*)*	*Maximum Value*	*Median Value*
Width at the midpoint	0.925 ± 0.585	0.4	3.6	0.8
Width at the external aperture	1.112 ± 0.801	0.5	5.5	1.0
Length	5.799 ± 3.262	1.2	17.5	5.4
Total	*Mean ± SD*	*Minimum Value (*)*	*Maximum Value*	*Median Value*
Width at the midpoint	0.902 ± 0.566	0.4	3.6	0.8
Width at the external aperture	1.169 ± 0.884	0.4	6.1	1.0
Length	5.669 ± 3.061	1.2	17.5	5.4

(*) Not visualized VA were excluded from counting.

Table 2 Qualitative assessment of the vestibular aqueduct

Grade	*Right Side*	*%*	*Left Side*	*%*	*Total*	*%*
0 - Not visualized	5	5.7	5	5.7	10	5.7
1 - Narrow	18	20.5	13	14.8	31	17.6
2 - Normal	54	61.4	61	69.3	115	65.3
3 - Borderline	3	3.4	3	3.4	6	3.4
4 - Enlarged	8	9.0	6	6.8	14	8.0

Table 3 External aperture morphology

Morphology	*Right Side*	*%*	*Left Side*	*%*	*Total*	*%*
Filiform	16	18.2	18	20.5	34	19.3
Tubular	47	53.4	47	53.4	94	53.4
Funnel-shaped	20	22.7	18	20.5	38	21.6
Not visualized	5	5.7	5	5.7	10	5.7

Table 4 Temporal bone pneumatizzation patterns

Type	*Right Side*	*%*	*Left Side*	*%*	*Total*	*%*
Type I	5	5.7	4	4.5	9	5.1
Type II	6	6.8	7	8.0	13	7.4
Type III	6	6.8	4	4.5	10	5.7
Type IV	33	37.5	34	38.6	67	38.0
Type V	38	43.2	39	44.4	77	43.8

Table 5 Jugular bulb

	Right Side	*%*	*Left Side*	*%*	*Total*	*%*
Normal	53	56.8	63	71.6	129	73.3
Enlarged / Ectasic	26	33	18	20.5	32	18.2
Dehiscence with the VA	8	9	7	7.9	14	7.9
Dehiscence with the CA	1	1.2	1*	0	1	0.6

(*) Only in one case was found a dehiscence with both the VA and CA.

Table 6 Distance between JB and the posterior canal bony wall (mm)

	Mean ± SD	*Minimum Value*	*Maximum Value*
Right Side	5.8 ± 3.5	0.2	13.8
Left Side	5.8 ± 3.7	0.2	12.9

Table 7 Evaluation of the osseous capsule covering the semicircular canals

	Right Side	*%*	*Left Side*	*%*	*Total*	*%*
Normal thickness	65	73.9	65	73.9	130	73.9
Reduced thickness	15	17.1	16	18.2	31	17.6
Dehiscence	8	9.0	7	7.9	15	

no association between VA length and the remaining parameters.

The evaluation of squamo-petro-mastoid aircells demonstrated a prevalence of a high degree of temporal bone pneumatization (81.8 %), with symmetry between the right and left sides (Pcc = 0.80, $p<0.0001$) Table 4.

Analyzing the relationship between JB and the CA or the VA, we found in 14 ears a dehiscence of the JB with the VA, in one ear with the CA and in one case a dehiscence with both the VA and the CA was found (Tables 5 and 6).

CT identified an abnormality of the bony overlay of the semicircular canals in 45 cases, showing 15 semicircular canal dehiscences and in 31 temporal bones a marked thinning of the bony overlay (Table 7). In all these cases bony defects, detected on axial CT scans, were confirmed on the coronal and min-IP reformatted images.

Clinical results

All six patients with enlarged vestibular aqueduct syndromes (EVAS or Class 3) had a suspected third window pathology and showed a VA wider than 1.5 mm on CT scans. Moreover CT identified four patients with large VA and ill-defined clinical symptoms, three of whom clinically suspected to be SNHL and one 1 BPPV.

In patients with BPPV (11 patients, Class 1) no VA abnormalities were found on CT scans, confirming the clinical diagnosis in ten patients; the remaining patient had an enlarged VA (EVAS), not clinically suspected

In the RV class (eight patients, Class 2) we found three patients with negative CT scans, two patients with a narrow aqueduct and subsequently reclassified as Ménière's disease patients, and three patients with ectasic JB dehiscence with the VA.

In patients suffering from sudden or progressive unilateral sensorineural hearing loss (Class 4, 18 patients) no statistically significant correlation was found with the morphological abnormalities. This result was expected since it is a clinical class characterized by extreme etiological heterogeneity.

CT identified an abnormality of the bony overlay of the semicircular canals in 45 ears, showing 15 semicircular canal dehiscences and in 30 temporal bones a marked thinning of the bony overlay. In 17 patients the alterations of the semicircular canals were found bilaterally and in seven of these patients there was a dehiscence from both sides. In all these cases bony defects, detected on axial CT scans, were confirmed on the coronal and min-IP reformatted images.

In patients with suspected pathology of the third window we did not find any case of dehiscence of the posterior semicircular canal or dehiscence of the basal turn of the cochlea.

The clinical suspicion of SSCD (Class 5) was confirmed by CT in 11/13 patients (84.6 %). In addition another seven patients showed a thinning or dehiscence of the superior semicircular canals as the prevailing alteration on CT scans, and were reclassified as pathology of the third window.

In Class 6 (25 patients) Ménière's disease symptoms were correlated with a VA alteration in more than half of the cases; the most striking finding in this class was that the VA was significantly narrower or related to a different functional narrowing condition compared with other classes, as demonstrated by detection of a narrow or not visualized VA in 21 patients (13 narrow VA and eight not visualized VA).

Discussion

Radiological investigations have always played a key role in the diagnostic assessment of vestibulocochlear diseases. The identification

of newly discovered vestibulocochlear patterns such as labyrinthine capsule dehiscence, the higher definition of inner ear malformations like the aqueductal malformations, and the increased need to improve the clinical differential diagnosis of disorders such as Ménière's disease or BPPV, have contributed to reassess the role of CT, that is today considered the most important imaging examination for audiological diagnostic interpretation.

The significant technological improvements of MDTC allow an accurate evaluation of the middle and inner ear structure morphology, with the possibility to investigate the anatomical relationships with dural or vascular components. Our study showed that MDCT is highly reliable not only in confirming the clinical suspicion but also in the differential diagnosis of non-unique clinical interpretation patients.

A close correspondence was found between the morphology of labyrinthine structures and the functional alteration clinically detected. This is more evident in some pathological conditions such as VA enlargement, dehiscence of the semicircular canals or in Ménière's disease where a predominance of restricted or not visualized forms of VA was observed.MDCT has also provided insights on the pathogenetic mechanisms underlying some vestibulocochlear conditions characterized by multifactorial etiology. The finding of an association between cases of vestibule-cochlear symptoms, not included in well-known audiological disorders, and conditions of anatomical contiguity between inner ear structures and vascular structures has recently led to new etio-pathophysiological hypotheses or a reevaluation of past etiological theories.

In patients with BPPV we observed that a high degree of pneumatization of the temporal bone could induce a condition of altered thermal, mechanical and acoustic insulation which would favor the otolith detachment.

In subjects with undefined recurrent vertigo, a direct contact between the VA and the jugular bulb could lead to an alteration of drainage or direction of endolymphatic flow, according to the congestion of the venous intracranial system.

The absence of a significant correlation between morphological abnormalities and symptoms in the group of sudden or progressive unilateral SNHL was nevertheless an expected result since it is a clinical class characterized by extreme etiological heterogeneity. In sudden or progressive SNHL the detection of four cases of enlarged VA and six cases of narrowed VA suggests the importance of MDCT scans in these patients, despite of the absence of precise correlations with the clinical and epidemiological information. Furthermore a narrowed VA supports the hypothesis that an impediment to longitudinal endolymph flow represents the cause or a contributing factor for the onset of hearing loss.

Conclusion

The study demonstrates that alterations of VA morphology are not only related to EVAS but are also found in other inner ear pathologies such as Ménière's disease. Furthermore MDCT may confirm correlations between the morphology of inner ear structures such as VA, semicircular canals or JB dehiscence, and alterations of vestibule-cochlear function, confirming the role of MDCT as the primary technique for understanding the mechanisms that regulate the functioning of the vestibule-cochlear system.

However, the interpretation of imaging in patients with cochleovestibular diseases remains a challenge because the etiology is often multifactorial and the correspondence between symptoms and anatomical alterations is not constant. The diagnostic accuracy achieved by MDCT allows a morphological characterization of the temporal bone with the possibility to obtain accurate measurements. The definition of reference values of inner ear structures can serve as an aid for CT images interpretation. Our study may provide a basis for further evaluations: by extending this method to more representative groups of patients normal morphometric ranges of inner ear components could be defined.

References

1 Krombach GA, van den Boom M, Di Martino E, et al. Computed tomography of the inner ear: size of anatomical structures in the normal temporal bone and in the temporal bone of patients with Ménière's disease. Eur Radiol. 2005; 15: 1505-1513. [PubMed: 15824909].
2 Atkin JS, Grimmer JF, Hedlund, G, et al. Cochlear abnormalities associated with enlarged vestibular aqueduct anomaly. Int J Pediatr Otorhinolaryngol. 2009; 73 (12): 1682-1685. [PubMed: 19775757].
3 Legeais M, Haguenoer K, Cottier JP, et al. Can a fixed measure serve as a pertinent diagnostic criterion for large vestibular aqueduct in children? Pediatr Radiol. 2006; 36: 1037-1042. [PubMed: 16865391].
4 Yuen HY, Ahuja AT, Wong KT, et al. Computed tomography of common congenital lesions of the temporal bone. Clin Radiol. 2003; 58: 687-693. [PubMed: 12943639].
5 Lemmerling MM, Mancuso AA, Antonelli PJ, et al. Normal modiolus: CT appearance in patients with a large vestibular aqueduct. Radiology. 1997; 204: 213-219. [PubMed: 9205250].
6 Marques SR, Smith RL, Isotani S, et al. Morphological analysis of the vestibular aqueduct by computerized tomography images. Eur J Radiol. 2007; 61: 79-83. [PubMed: 17049195].
7 Koesling S, Rasinski C, Amaya B. Imaging and clinical findings in large endolymphatic duct and sac syndrome. Eur J Radiol. 2006; 57: 54-62. [PubMed: 16289429].
8 Dimopoulos PA, Smedby O, Wilbrand HF. Anatomical variations of the human vestibular aqueduct. Part I. A radioanatomical study. Acta Radiol Suppl. 1996; 403: 21-32. [PubMed: 8669309].
9 Clemis JD, Valvassori GE. Recent radiographic and clinical observation on vestibular aqueduct (a preliminary report). Otolaryngol Clin N Am. 1968; 1: 339-346.
10 Lo William WM, Daniels David L, Chakeres Donald W, et al. The endolymphatic duct and sac. Am J Neuroradiol. 1997; 18: 881-887. [PubMed: 9159365].
11 Valvassori GE, Clemis JD. The large vestibular acqueduct syndrome. Laryngoscope. 1978; 88: 723-728. [PubMed: 306012].
12 Tanioka H, Zusho H, Machida T, et al. High resolution MR imaging of the inner ear: findings in Ménière's disease. Eur J Radiol. 1992; 15: 83-88. [PubMed: 1396797].
13 Yamamoto E, Mizukami C, Isono M, et al. Observation of the external aperture of the vestibular aqueduct using three-dimensional surface reconstruction imaging. Laryngoscope. 1991; 101: 480-483. [PubMed: 2030626].
14 Purcell DD, Fischbein N, Lalwani AK. Identification of previously "undetectable" abnormalities of the bony labyrinth with computed tomography measurement. Laryngoscope. 2003; 113: 1908-1911. [PubMed: 14603045].
15 Committee on Hearing and Equilibrium guidelines for the diagnosis and evaluation of therapy in Ménière's disease. American Academy of Otolaryngology-Head and Neck Foundation, Inc. Otolaryngol Head Neck Surg. 1995; 113: 181-185. [PubMed: 7675476].
16 Lempert T. Vestibular migraine. Semin Neurol. 2013; 33: 212-218. [PubMed: 24057824].
17 Valvassori GE. Laminagraphy of the ear: normal roentgenographic anatomy. Am J Roentgenol Radium Ther Nucl Med. 1963; 89: 1155-1167. [PubMed: 13995951].
18 Buckingham RA, Valvassori GE. Tomographic anatomy of the temporal bone. Otolaryngol Clin North Am. 1973; 6 (2): 337-362. [PubMed: 4220297].
19 Ozgen B, Cunnane ME, Caruso PA, et al. Comparison of 45° oblique reformats with axial reformats in CT evaluation of the vestibular aqueduct, Am J Neuroradiol. 2008; 29 (1): 30-34. [PubMed: 17947373].

Dr Vincenzo Maiolo
Radiology Department
S.Orsola-Malpighi University Hospital
Via Massarenti, 9
40126 Bologna, Italy
E-mail: maiolo.vincenzo@yahoo.it